

# Co-published by Institute of Fluid-Flow Machinery Polish Academy of Sciences

#### **Committee on Thermodynamics and Combustion**

Polish Academy of Sciences

Copyright©2025 by the Authors under licence CC BY-NC-ND 4.0

http://www.imp.gda.pl/archives-of-thermodynamics/



# Online monitoring of thermal loads of steam turbine components

Mariusz Banaszkiewicz

Institute of Fluid-Flow Machinery, Polish Academy of Sciences, Energy Conversion Department, ul. Fiszera 14, 80-231 Gdańsk, Poland Author email: mbanaszkiewicz@imp.gda.pl

Received: 05.02.2025; revised: 04.06.2025; accepted: 11.06.2025

#### **Abstract**

The increasing share of renewable energy production in energy markets has resulted in the demand for more flexible operation of conventional power plants. Coal-fired units are forced to operate in a more cyclic duty with a higher number of starts, faster start-ups and increased load change rates. These unfavourable operating conditions result in additional thermal loading of steam turbine components and necessitate better monitoring of life-limiting components. The paper presents numerical investigations of thermal loading of a steam turbine valve at various operating conditions and identifies the requirements for an online monitoring method. A modified method based on Duhamel's integral is proposed and validated at different transient conditions, taking into account both convection and condensation heat transfer. It was shown that the calculation method provides reasonably accurate predictions of casing wall temperature. Relative differences between measured and calculated wall temperatures are within  $(-2.6\%) \div (+1.5\%)$  for the investigated start-ups with condensation and convection heat transfer conditions. Advantages of this method and its suitability for online monitoring of thermal loads of steam turbine components are discussed in detail.

Keywords: Steam turbine; Thermal loads; Condensation; Duhamel's integral

Vol. 46(2025), No. 3, 5–15; doi: 10.24425/ather.2025.154920

Cite this manuscript as: Banaszkiewicz, M. (2025). Online monitoring of thermal loads of steam turbine components. *Archives of Thermodynamics*, 46(3), 5–15.

#### 1. Introduction

The demand for more flexible operation of conventional power plants has significantly increased during the last years. The typical operation mode of coal fired plants has shifted from a more base load oriented regime towards cyclic operation. This is due to the increasing share of fluctuating renewable energy production [1].

Consequences of this trend are an increased number of starts, faster start-ups and increased load change rates. Additionally, the minimum load for stable plant operation has to be reduced to allow low load operation of conventional units. As a result of these changes in operation mode, thermal fatigue of power plant

equipment has become the main damage mechanism, which could potentially lead to component failures. This problem mainly affects the thick-walled components operating at high temperatures, like steam turbine rotors or valve casings.

In order to ensure safe and reliable operation of ageing power generation units, online monitoring of critical components has become necessary. In particular, for better understanding of the effect of changed operation mode on low cycle fatigue damage, accurate monitoring of thermal loads and stresses is essential.

The problem of thermal stress and load modelling for online monitoring of power plant equipment has been studied for many years, but has gained particular attention in recent years. Rusin et al. [2–4] proposed a new method of thermal stress modelling

#### **Nomenclature**

Bi - Biot number

 $c_p$  – specific heat,  $J/(kg \cdot K)$ 

d – hydraulic diameter, m

g – heat source,  $J/(m^3 \cdot s)$ 

h – enthalpy, J/kg

H – Heaviside function,

L – length, m

Nu-Nusselt number

p – pressure, kPa

Pr - Prandtl number

r - radial co-ordinate, m

Re - Reynolds number

t - time, s

T – temperature, K

#### **Greek symbols**

 $\alpha$  – heat transfer coefficient, W/(m<sup>2</sup>·K)

in turbine rotors employing Green's functions and Duhamel's integral, and steam temperature measurement at a critical location. Such an approach has also been adopted for monitoring of power boilers operation by Taler et al. [5], and as shown by Lee et al. [6], it can also be used for calculating stress intensity factors at transient thermal loads.

The major issue in using Green's function and Duhamel's integral method to model transient temperatures and thermal stresses in steam turbine components is the time-dependence of physical properties and heat transfer coefficients, affecting the proper evaluation of Green's functions. There are known approaches assuming determination of the influence functions at constant values of these quantities [7]. The inclusion of temperature dependent physical properties proposed by Koo et al. [8] relies on determining the weight functions for steady-state and transient operating conditions. A more important, in most cases, variation of the heat transfer coefficient can be taken into account by calculating the surface temperature using a reduced heat transfer model and employing Green's function to calculate stress response to a step change of metal surface temperature [9]. However, numerical solution of a multi-dimensional heat transfer model is complicated and time-consuming, and due to this, it cannot be used in online calculations. A full inclusion of time variability of the physical properties and heat transfer coefficients proposed by Zhang et al. [10] relies on the solution of a non-linear heat conduction problem by using the artificial parameter method and superposition rule, and replacing the timedependent heat transfer coefficient with a constant value together with a modified fluid temperature. The effectiveness of the method has been proved by an example of a three-dimensional model of pressure vessel of a nuclear reactor.

Alternative methods of thermal stress modelling rely on using artificial neural networks [11–13] or inverse heat conduction methods [14–17]. Some researchers [18,19] investigated an approach combining direct heat conduction problems and Duhamel's integral.

This work presents numerical investigations of thermal loading of a steam turbine valve and proposes a modified method for

 $\lambda$  – thermal conductivity, W/(m·K)

 $\xi$  – friction factor

 $\rho$  – density, kg/m<sup>3</sup>

#### **Subscripts and Superscripts**

a – air

cond-condensation

conv-convection

f - fluid

n – time step number

sat - saturation

st - steam

surf-surface

w – wall

#### **Abbreviations and Acronyms**

FEM - finite element method

HS - hot start

WS - warm start

online monitoring of wall temperature employing Duhamel's integral. The main attention is given to appropriate consideration of different heat transfer mechanisms (condensation, convection) and determination of the temperature response function for a variable heat transfer coefficient. The proposed method is validated with the help of real measurements of casing wall temperature and finite element calculations.

## 2. Finite element modelling of turbine valve heating process

#### 2.1. Problem formulation

The problem under consideration is transient heat conduction in a homogeneous isotropic solid described by the Fourier-Kirchhoff differential equation [20,21]:

$$\operatorname{div}[\lambda \operatorname{grad}T(\boldsymbol{r},t)] + g(\boldsymbol{r},t) = \rho c_p \frac{\partial T(\boldsymbol{r},t)}{\partial t}, \tag{1}$$

where T is the metal temperature, g is the heat source,  $c_p$  is the specific heat,  $\lambda$  is the thermal conductivity and r is the spatial location.

Neglecting the heat source g and introducing the temperature Laplacian  $\nabla^2 T$ , Eq. (1) is rewritten in a rectangular co-ordinate system as follows:

$$\rho c_p \frac{\partial T}{\partial t} = \lambda \nabla^2 T + \frac{\partial \lambda}{\partial T} \left( \left( \frac{\partial T}{\partial x} \right)^2 + \left( \frac{\partial T}{\partial y} \right)^2 + \left( \frac{\partial T}{\partial z} \right)^2 \right). \tag{2}$$

In a rectangular co-ordinate system, the temperature Laplacian is defined as follows:

$$\nabla^2 T = \frac{\partial^2 T}{\partial x^2} + \frac{\partial^2 T}{\partial y^2} + \frac{\partial^2 T}{\partial z^2}.$$
 (3)

A uniform temperature distribution  $T(\mathbf{r}) = T_0$  is assumed as an initial condition at t = 0.

For the turbine valve casings, the following boundary condition is applied:

$$\lambda \frac{\partial T}{\partial n}\Big|_{s} = -\alpha \left(T_{surf} - T_{st}\right) \text{ for } t \ge 0,$$
 (4)

where n denotes the normal direction to the surface,  $T_{surf}$  is the surface temperature,  $T_{st}$  is the steam temperature and  $\alpha$  is the heat transfer coefficient.

The Fourier-Kirchhoff Eq. (2) is solved by means of the finite element method [22].

#### 2.2. Heat transfer coefficients

The variation of heat transfer coefficient  $\alpha(t)$  is considered by the Nusselt number Nu changing in time as a function of the Reynolds number Re and Prandtl number Pr:

$$Nu = f(Re, Pr). (5)$$

The Nusselt number is defined as follows:

$$Nu = \frac{\alpha d}{\lambda}, \qquad (6)$$

where d denotes the hydraulic diameter.

The detailed form of Eq. (5) depends on the component geometry and flow character [23]. Practical methods of determining heat transfer coefficients are presented in [20]. The heat transfer model adopted in this study is based on the well-proven formulae for heat transfer coefficients in steam turbine components and can be employed in online calculations of temperatures and thermal stresses, which is not possible when more advanced thermal fluid-structure interaction (FSI) modelling is adopted [24-27]. Online calculations require fast and robust models which can be implemented and run on industrial computers. For typical start-up conditions and geometry of steam turbine components, the time constants of thermal processes require solving the model with new boundary conditions with a time step of around 1 minute. Start-up durations are in the range of 30 to 200 minutes, which are the required calculation times. Such times are achievable for the finite element method with convection or condensation boundary conditions, but for FSI calculations involving fluid flow and solid body simulations, these times can be several times longer. Moreover, iteration processes and time steps employed in FSI calculations adversely affect not only the calculation times but also stability and reliability of solutions. Such calculations require high performance computers while simple algorithms based for example on Duhamel's integral are easily implementable in programmable logic controllers (PLCs).

For the valve casing regions of circular cross-section, the Gnielinski correlation [28,29] is used:

$$Nu = \frac{\frac{\xi}{8} (Re - 1000) Pr}{1 + 12.7 \sqrt{\frac{\xi}{9} (Pr^{2/3} - 1)}} \left[ 1 + \left( \frac{d}{L} \right)^{2/3} \right] \left( \frac{Pr_m}{Pr_w} \right)^{0.11}, \tag{7}$$

where L is the pipe length and symbol  $\xi$  denotes the friction factor, for smooth tubes calculated from Filonienko's formula [30]:

$$\xi = \frac{1}{(1.82\log\text{Re} - 1.64)^2}.$$
 (8)

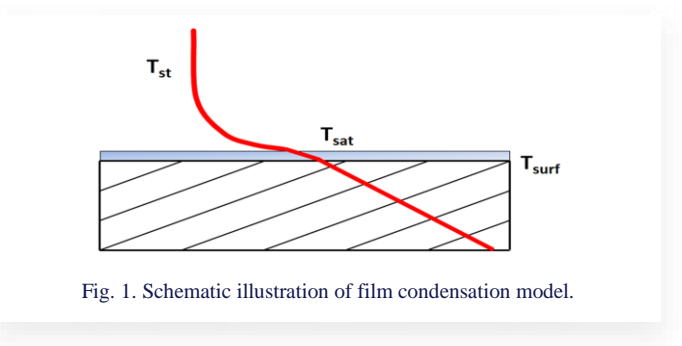
The symbols  $Pr_m$  and  $Pr_w$  designate the Prandtl number at the bulk and wall, respectively.

For the valve main chamber, a simple power-law formula similar to those of Dittus-Boelter [31–33] and Chilton-Colburn [34] correlations is applied:

$$Nu = 0.018Re^{0.8}Pr^{0.33}$$
. (9)

The factor 0.018 was established based on 3-dimensional thermal fluid-solid interaction calculations performed for this valve with time-dependent boundary conditions representing valve heating up from a cold, warm and hot state [35]. Direct simulation results using a 3-dimensional FSI method were available for design start-up conditions, assuming theoretical variations of steam temperature, pressure and mass flow rates. The primary goal of these calculations was to determine a relationship between the similarity numbers (i.e. Nusselt and Reynolds numbers) for the analysed valve geometry, which could be used in finite element calculations and online calculations for any start-up conditions (not only for the predefined design start-ups).

When the turbine starts from a cold state or during pre-warming, steam condensation can take place on valve casing inner surfaces, and condensation heat transfer should be taken into account. Steam condensation on casing surfaces can occur when steam is superheated or saturated. The film condensation mechanism is assumed. A schematic illustration of the condensation model adopted in this work is shown in Fig. 1. If the surface temperature is lower than the saturated steam temperature at the corresponding steam pressure, then steam condenses on the surface. The heat transfer to the surface is intensified as a result of water films appearing on the surface at the saturated steam temperature and the heat released due to condensation.



Condensation occurs if the following conditions are satisfied [36]:

- the metal temperature is below the saturation temperature  $T_{sat}$  at the local pressure p:

$$T_{sat} > T_{surf},$$
 (10)

 the heat flux from water film to metal is greater than the heat flux from steam to water film:

$$\alpha_{cond} \big( T_{sat} - T_{surf} \big) > \alpha_{conv} (T_{st} - T_{sat}). \tag{11}$$

As concluded in [23], available correlations for the Nusselt number for simple geometries, like a flat wall or pipe, can be used for estimating the condensation heat transfer coefficient usually with a large error. However, it is known that heat transfer coefficients during steam condensation assume large values reaching 120 000 W/( $m^2$ ·K) in extreme cases during nucleate condensation of steam [37,38] and, consequently, the errors of their estimation will only slightly affect the variations of temperature and thermal stress fields in turbine components. It was shown that for Biot numbers Bi > 20, the variation of heat trans-

fer coefficient has little influence on the variation of temperature distribution [23]. Due to the lack of proper correlations for real turbine geometries and taking into account the above conclusions, the analyses of condensation heat transfer were performed with a constant heat transfer coefficient  $\alpha = 11~000~\text{W/(m^2 \cdot \text{K})}$ . This value is within the range of heat transfer coefficients predicted by Shah [39] for film condensation of water inside pipes.

#### 2.3. Numerical results and model validation

For numerical calculations of valve heating-up, a three dimensional model has been prepared. The model includes half of the valve due to the symmetry of valve geometry and flow conditions (Fig. 2). Steam enters the valve through the inlet pipe and flows into the main chamber where the flow changes direction from horizontal to vertical. Further steam flows through a converging-diverging channel and leaves the valve through the outlet pipe. Wall temperature measurement is installed in the main chamber region in the wall section perpendicular to the inlet pipe axis and containing the outlet pipe axis. The measurement point is located at a 10 mm distance from the wall inner surface where the hot junction of the measuring thermocouple is located.

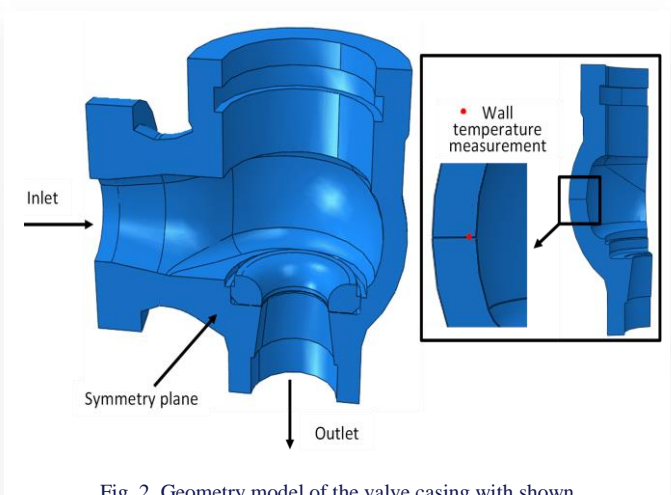


Fig. 2. Geometry model of the valve casing with shown wall temperature measurement location.

Numerical calculations have been performed using the Abaqus code [40]. Computational mesh size was approximately 94 000 second order diffusion elements with 89 546 tetrahedral and 4459 hexahedral elements. Casing material is heat resistant cast steel GS-17 CrMoV 5 11, and its physical properties as a function of temperature are given in Table 1 [35,41]. The cast steel density is constant and equal to 7850 kg/m<sup>3</sup>.

Table 1. Physical properties of GS-17 CrMoV 5 11 cast steel at different temperatures.

Temperature, T [°C]	20	100	200	300	400	500	550
Thermal conductivity, $\lambda$ [W/(m·K)]	50	47	46	44	41	39	37
Specific heat, c <sub>ρ</sub> [kJ/(kg·K)]	0.46	0.49	0.53	0.57	0.61	0.68	0.73

Fig. 3 presents inlet steam parameters for the warm start-up with pre-warming, together with the rotor rotational speed and

turbine load. Pre-warming is conducted by supplying steam to the valve chamber when the valve is in the closed position and evacuating condensate through a drain. Valve pre-warming takes place for 85 minutes until stop and control valves start to open. For the first 25 minutes, steam is at saturation and afterwards becomes superheated. During run-up and loading, the steam temperature and superheating increase, and reach maximum values at full load.

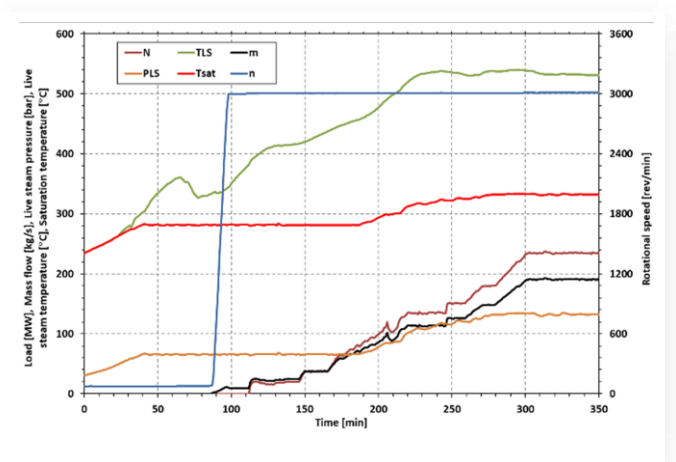
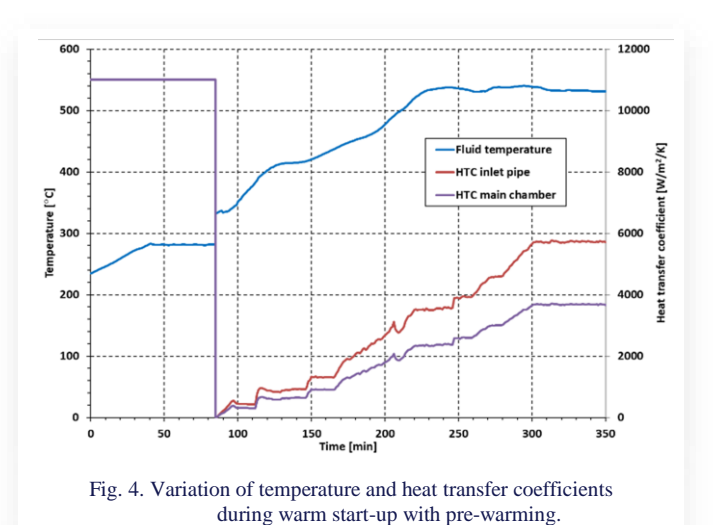


Fig. 3. Variation of inlet steam parameters, rotational speed and load during warm start-up with pre-warming.

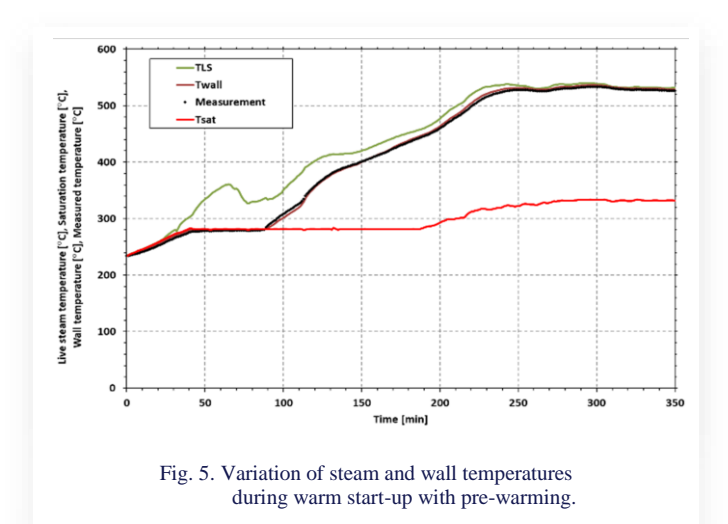
A constant temperature of the valve casing equal to 240°C was assumed as an initial condition. Start-up simulations were carried out with time-dependent Fourier boundary conditions. Variation of fluid temperature and heat transfer coefficients for the inlet pipe and valve main chamber is presented in Fig. 4.



The calculated wall temperature at the measurement point is compared with the measured temperature in Fig. 5, which also presents steam and saturation temperatures. It is seen that the calculated wall temperature closely follows the measured value both during valve pre-warming and during start-up. The maximum deviation calculated as:

$$Deviation = \frac{Predicted T_{wall} - Measured T_{wall}}{Measured T_{wall}}, \qquad (12)$$

does not exceed 1.5% during pre-warming and -2.6% during steam heating.



It is noted that condensation heat transfer prevails during the whole pre-warming phase until the beginning of run-up, and the wall temperature follows the saturation temperature. In early phases steam condensation on the valve inner surfaces takes place with saturated steam conditions and continues with superheated steam even for superheating reaching 80°C. When the valves start to open, the superheated steam flow through the valve brings about intensified heating of the valve and the wall temperature starts to increase above the saturation temperature. Since then, the casing temperatures continuously increase, slowly approaching the live steam temperature and departing the saturation temperature.

Temperature distributions in the valve casing at various phases of pre-warming and steam heating are shown in Figs. 6

and 7, respectively. Uniform temperature distribution was assumed as an initial condition for pre-warming (Fig. 6a). The first 20 minutes of pre-warming proceeds with saturated steam which condenses on the inner surfaces of the inlet pipe and main chamber. The wall surface temperature in these regions reaches 255°C (Fig. 6b), and the remaining regions are still at temperatures close to the initial. Further pre-warming takes place with superheated steam, and after 40 minutes, the wall surface temperature attains ~281°C (saturation temperature, Fig. 6c). After this time, considerable differences between surface temperature where condensation takes place and temperatures of remaining regions are still present. At the end of the pre-warming phase (Fig. 6d), temperature distribution becomes more uniform because the valve sections not being in contact with condensing steam are already heated-up via convection.

After 85 minutes of pre-warming, turbine run-up begins and steam starts to flow through the valve, bringing about intensive heating of the valve casing. The wall temperature reaches approximately 400°C after 60 minutes (Fig. 7a) and almost 500°C after 120 minutes (Fig. 7b) since the beginning of run-up. It should be noted that during the initial phases of steam heating, the temperatures of valve inlet and outlet regions tend to equalise as both regions are heated with comparable intensity by steam flow through the open valve. After 180 minutes, the nominal steam temperature is attained and the major part of the casing is at a temperature above 500°C (Fig. 7c). Since then, the temperature field is becoming more uniform while the inner surfaces being in contact with steam remain at almost constant temperature (Fig. 7d).

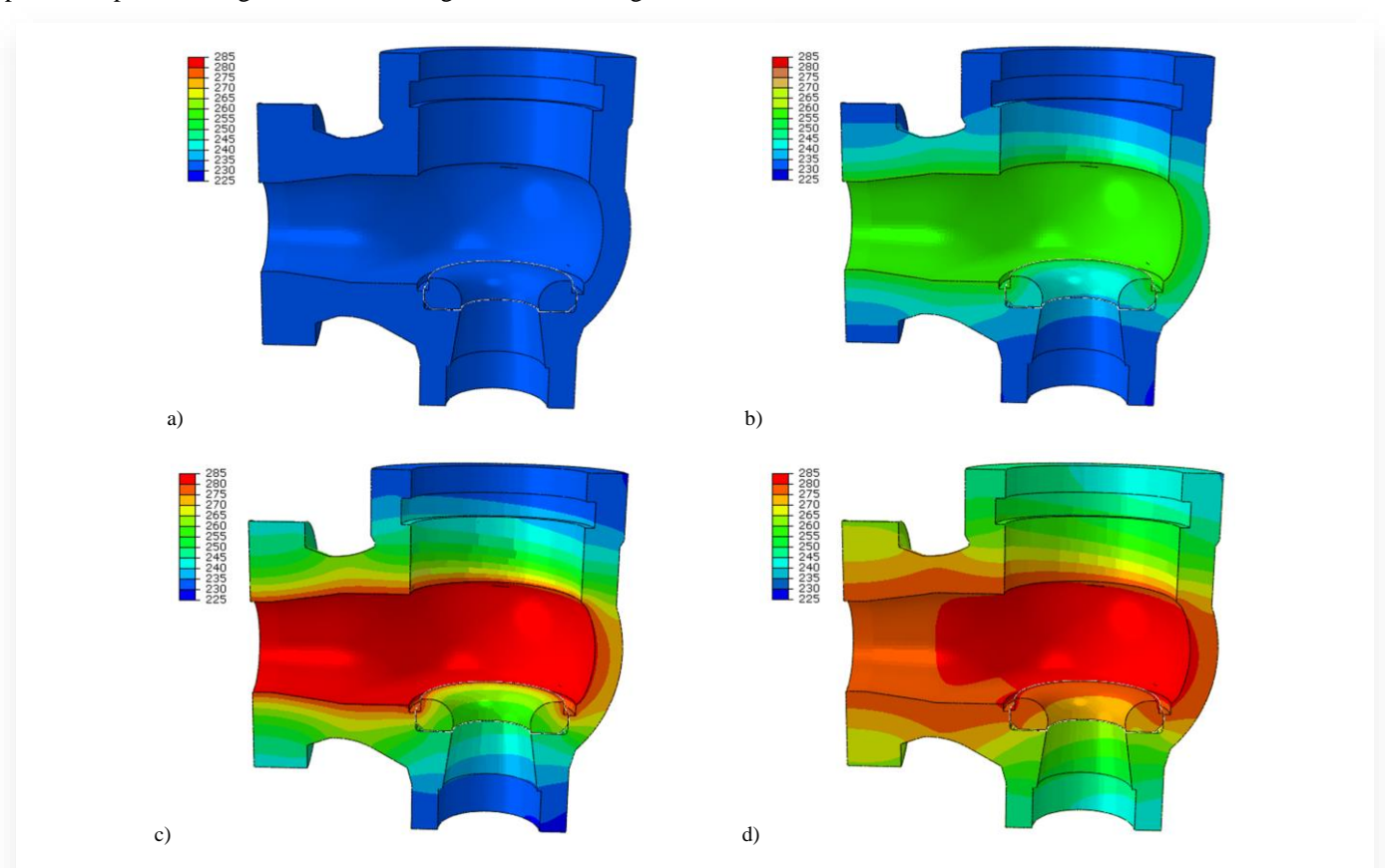


Fig. 6. Temperature distribution in the valve casing at various phases of pre-warming: a) t = 0 min, b) t = 20 min, c) t = 40 min, d) t = 85 min.

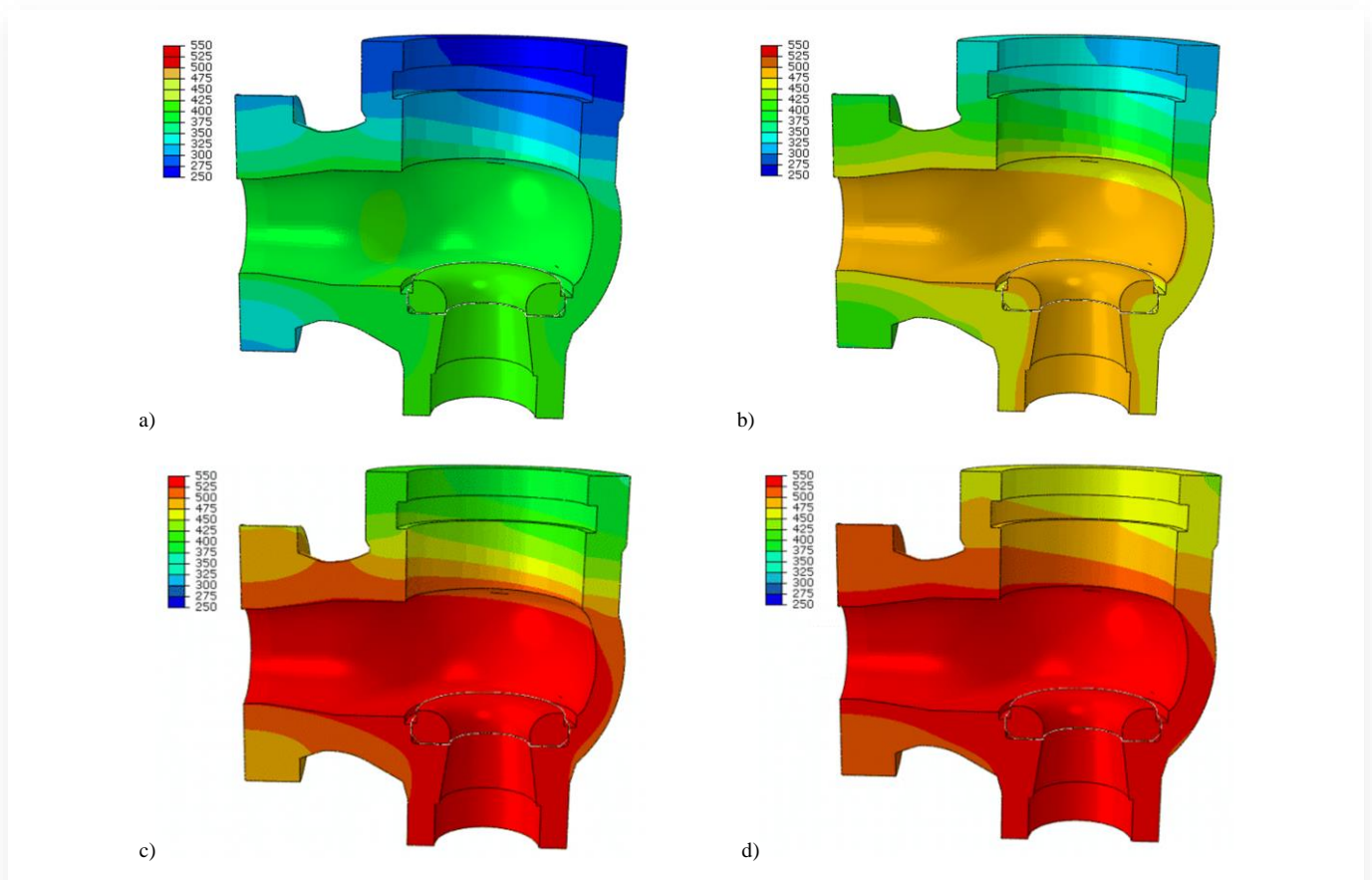


Fig. 7. Temperature distribution in the valve casing at various phases of steam heating: a) t = 60 min, b) t = 120 min, c) t = 180 min, d) t = 240 min.

#### 3. Duhamel's integral method

#### 3.1. Theoretical background

Duhamel's integral can be used for determining the temperature distribution in the body. For steam turbine components, a reliable and accurate measurement of surface temperature at the critical region is usually not possible, thus for on-line monitoring purposes, steam temperature measurement is used as a leading signal. Consequently, in the heat transfer model, Fourier's boundary condition (4) is applied.

Assuming that the steam temperature is described by Heavi-side's function H(t) [10], [42]

$$H(t) = \begin{cases} 0, & t < 0 \\ 1, & t > 0 \end{cases}$$
 (13)

the boundary condition (4) can be written in the form [10]:

$$\lambda \frac{\partial X}{\partial n} = -\alpha \big( H(t) - X(r, t) \big), \tag{14}$$

where  $X(\mathbf{r}, t)$  is a solution of the direct heat conduction problem with a unit step change of steam temperature.

Using the solution  $X(\mathbf{r}, t)$ , we can calculate metal temperature for an arbitrary variation of steam temperature employing Duhamel's theorem [43]:

$$T(\mathbf{r},t) = T_0 + \int_0^t X(\mathbf{r},t-\tau) \frac{\partial T_{St}(\tau)}{\partial \tau} d\tau.$$
 (15)

For simple geometries like a plate, cylinder or sphere, a solu-

tion of the one-dimensional transient heat conduction problem can be obtained analytically. In the case of more complex shapes, it is necessary to use numerical methods, e.g. the finite element method in order to obtain accurate solutions.

#### 3.2. Numerical solution of Duhamel's integral

In order to solve Duhamel's integral given by Eq. (15), it is transformed from a continuous into discrete form:

$$T(\boldsymbol{r},t) = T_0 + \sum_{t-t_d}^t X_t(\boldsymbol{r},t-\tau) \Delta T_{st}(\tau) + X_s(\boldsymbol{r},t), \ (16)$$

where  $t_d$  is a cut-off time,  $X_s(\mathbf{r},t)$  is a value of the influence function in steady state, while  $X_t(\mathbf{r},t)$  is a transient part of the influence function.

In principle, Duhamel's integral, resulting from the superposition rule, can be applied to linear unsteady heat conduction problems. However, it has been shown in previous studies on thermal stress modelling using Duhamel's integral that it can be successfully applied to nonlinear thermoelasticity problems when the appropriately obtained solution of direct heat conduction problem  $X(\mathbf{r}, t)$  is used [42]. This solution is obtained numerically with the assumption of time-dependent heat transfer coefficients  $\alpha(t)$  and temperature-dependent specific heat  $c_p(T)$  and thermal conductivity  $\lambda(T)$ .

It has been shown in Section 2 that for adequate modelling of thermal behaviour of turbine valves, both condensation and convection heat transfer have to be taken into account. Insofar as the condensation heat transfer coefficient can be assumed constant and high, the convection heat transfer coefficient can vary by orders of magnitude during start-up. Equation (16) is then rewritten into the form:

$$T(\mathbf{r},t) = T_0 + \sum_{t-t_d}^t X_{t,cond}(\mathbf{r},t-\tau) \Delta T_{sat}(\tau) + k \sum_{t-t_d}^t X_{t,conv}(\mathbf{r},t-\tau) \Delta T_{st}(\tau) + X_s(\mathbf{r},t),$$
(17)

where  $X_{t,cond}$  is a temperature response function for condensation determined with a constant heat transfer coefficient,  $X_{t,conv}$  is a temperature response function for convection determined with a variable heat transfer coefficient and k is a factor responsible for compensating for nonlinearity of the problem. When necessary conditions for condensation are met, then  $\Delta T_{st} = 0$ , and when condensation vanishes, then  $\Delta T_{sat} = 0$ .

In steady state conditions, the two terms with summation over time tend to zero, and the steady state term  $X_s(\mathbf{r},t)$  is given by the following formula:

$$X(\mathbf{r},t) = 0.9 \left( T_{st}(t-t_d) - T(t-t_d) \right) \times \left( 1 + 0.1 exp\left( \frac{1}{t_d-t} \right) \right).$$
 (18)

This term is assumed to be zero at transient states and is activated and contributes to the calculation of temperature when nearly steady state conditions are reached.

#### 4. Validation of Duhamel's integral method

Validation of the proposed method based on Duhamel's integral and described by Eq. (17) was done by performing numerical calculations of wall temperature for three different start-ups using the proposed method. The results were then compared with real measurements of the valve casing temperature and predictions of the FEM model presented in Section 2.

### 4.1. Temperature response function for convection and condensation

The accuracy of the proposed method depends on the form of the temperature response function, which in turn is primarily determined by the variation of the heat transfer coefficient. As it has been previously shown, the condensation heat transfer coefficient can be assumed constant and good accuracy of temperature predictions is obtained with  $\alpha_{cond} = 11\ 000\ \text{W/(m}^2 \cdot \text{K)}$ . Figure 8 presents the temperature response functions for the wall surface and temperature measurement point located 10 mm below the surface. These functions were obtained using the finite element model of the valve presented in Section 2 and applying a step change of steam temperature from 125°C to 280°C. The temperature response was then related to the change of steam temperature (equal in this case to 155°C) to obtain a response function to a change of steam temperature by 1°C. In numerical simulations, material physical properties were temperature-dependent, and the heat transfer coefficient was kept constant.

Figure 8 also presents the temperature response functions for convection, which were obtained for variable heat transfer coefficients shown in Fig. 4. In this case, a step change of steam temperature from 280°C to 540°C was simulated, assuming temperature-dependent material properties. The shape of tempera-

ture response function reflects the variation in time of the heat transfer coefficient. It is seen from the figure that in condensation conditions, the temperature response is more rapid and regular than for convection. This behaviour results from the assumption of a constant and higher than for convection heat transfer coefficient during condensation.

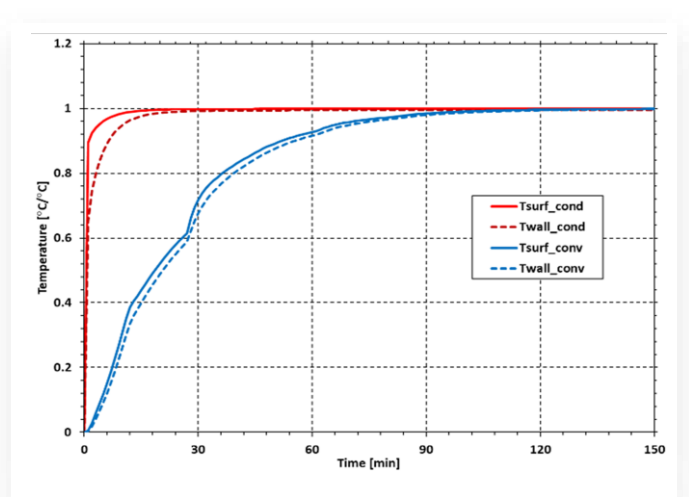


Fig. 8. Temperature response function for wall surface and measurement point location for condensation and convection.

## 4.2. Simulation of start-ups from various initial thermal states

The results of numerical calculations performed using Duhamel's integral were compared with wall temperature measurements and predictions of the finite element method for three different start-up conditions covering the whole range of turbine operation:

- i. pre-warming from a cold state (Fig. 9),
- ii. warm start with pre-warming (Fig. 10),
- iii. hot start (Fig. 11).

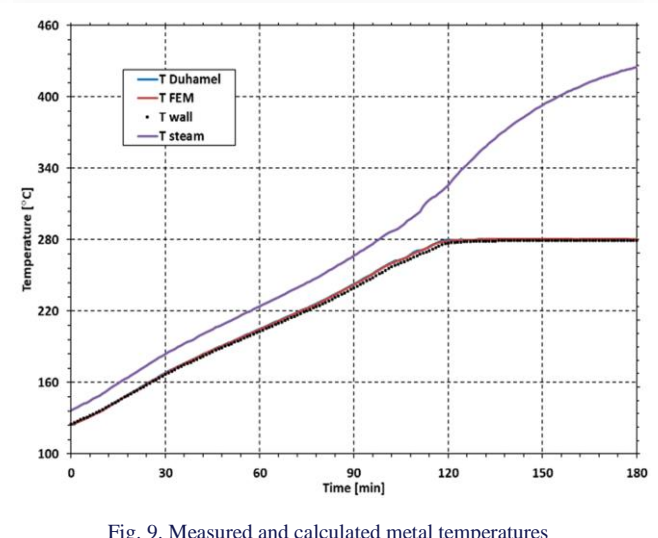


Fig. 9. Measured and calculated metal temperatures during pre-warming from a cold state.

In case i), steam condensation took place during the whole analysed period, while in case iii), only convection heat transfer was present. Case ii) included both condensation and convection. Steam condensation was modelled with the assumption of

#### Banaszkiewicz, M.

a constant heat transfer coefficient  $a_{cond} = 11\ 000\ \text{W/(m}^2 \cdot \text{K)}$ , while for forced convection, variable heat transfer coefficients were used. Thermal boundary conditions for warm start with pre-warming were presented in Fig. 4, while those calculated for the hot start are shown in Fig. 12. A constant temperature of the valve casing equal to 479°C was assumed as an initial condition for the hot start. The factor k = 1.12 accounting for nonlinearity of thermal boundary conditions was obtained by tuning for the warm start conditions and further used in hot start calculations.

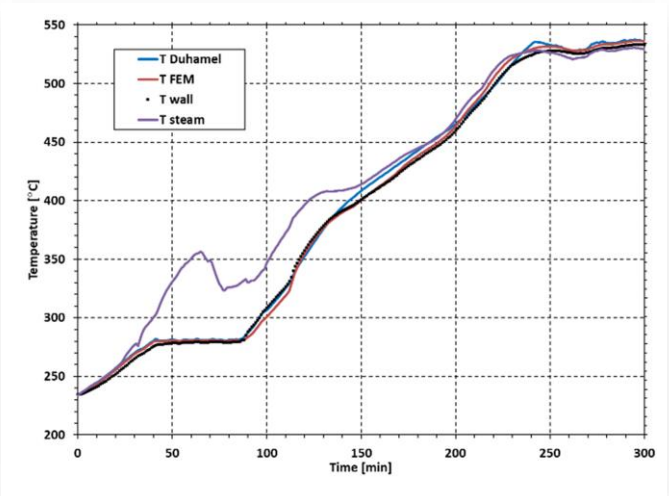


Fig. 10. Measured and calculated metal temperatures during warm start with pre-warming.

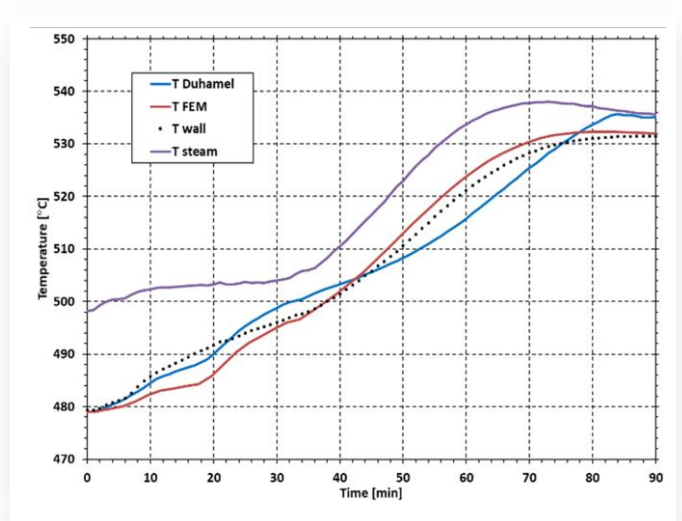
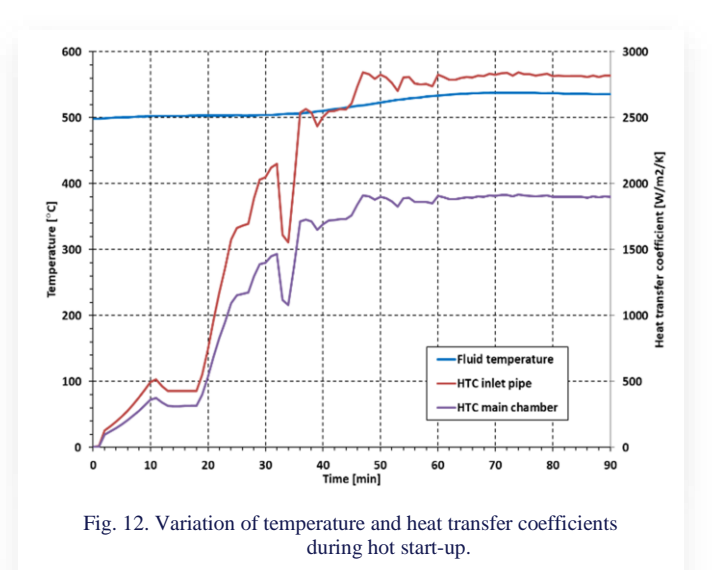


Fig. 11. Measured and calculated metal temperatures during hot start.

In all cases, very good agreement between calculations and measurements was found. At condensation conditions (Fig. 9 and Fig. 10), both methods (i.e. FEM and Duhamel's integral) predict nearly the same wall temperatures, which are very close to the measured temperature following steam saturation temperature. When the condensate film began to evaporate and convection heat transfer prevailed, larger deviations between calculated and measured temperatures were found. This is attributed mainly to inaccuracies in heat transfer coefficients determined with the help of simple correlations for pipe flows. However, the overall accuracy of the method based on Duhamel's integral can be assessed as high, taking into account the achieved deviations:

- i.  $(-1.0\%) \div (+1.5\%)$ ,
- ii. (-2.6%)÷(+1.5%),
- iii.  $(-1.0\%) \div (+0.8\%)$ .



Temperature differences are also observed between the two calculation methods, in particular for forced convection. The two simulated start-ups show that Duhamel's integral tends to predict higher temperatures than FEM at lower heat transfer coefficients (lower steam velocities) and lower temperatures at higher heat transfer coefficients. Nevertheless, it should be noted that the degree of agreement between the detailed FEM calculations and predictions of the simple Duhamel's integral method is satisfactory. Finite element modelling of such complex components with nonlinear thermal boundary conditions is time consuming and results in a large amount of output data. Its use for online monitoring of power plant equipment is still impractical. However, the simple method described by Eq. (17) is fast, robust, accurate and easy to implement in industrial controllers. It considers in a simplified way the complex geometry of turbine and boiler components as well as the nonlinearity of thermal boundary conditions resulting from variation of steam temperature and heat transfer coefficient. The satisfactory accuracy of Duhamel's integral makes it very useful for online monitoring of thermal loading of turbine and boiler components.

For online checking of condensation conditions given by Eqs. (10) and (11), the wall surface temperature  $T_{surf}$  is calculated with the help of Eq. (17) and the temperature response function for the wall surface. Figure 13 presents the comparison of this temperature obtained with the help of Duhamel's integral and FEM for the warm and hot start-up. Thermal boundary conditions for the warm start are presented in Fig. 14, while for the hot start, the conditions shown in Fig. 12 were used. A constant temperature of the valve casing equal to 279°C was assumed as an initial condition for the warm start. Also for the surface temperature, reasonably good agreement between the two methods is found, in particular in the early phases of start-ups. These phases are very important because steam condensation on the valve surface can occur at the beginning of start-ups, and accurate prediction of the surface temperature is crucial in detecting steam condensation.

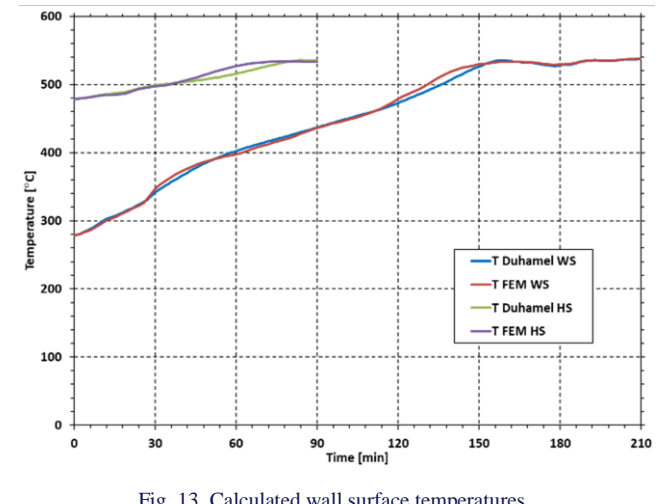


Fig. 13. Calculated wall surface temperatures during warm (WS) and hot start (HS).

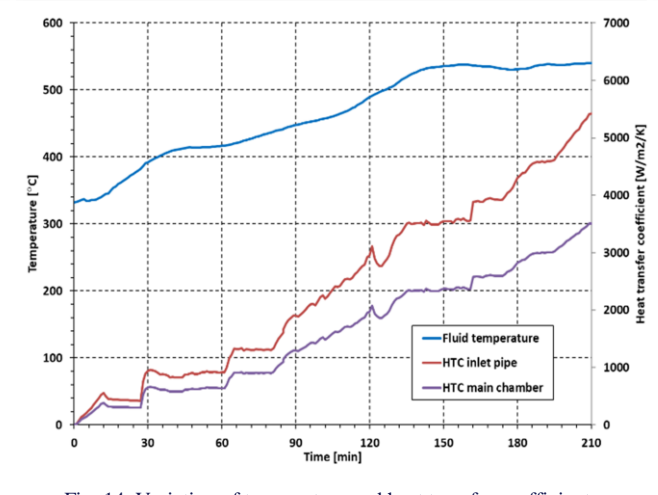


Fig. 14. Variation of temperature and heat transfer coefficients during warm start-up.

#### 5. Summary

The paper presented numerical investigations of thermal loading of the turbine valve at various operating conditions. These included pre-warming from a cold state, warm start with pre-warming and hot start-up. Both condensation and convection heat transfer mechanisms were modelled. In the finite element modelling, it was done by applying condensation and forced convection heat transfer coefficients to the valve surfaces in contact with steam.

The proposed method for online calculation of metal temperature is based on Duhamel's integral. Different mechanisms of heat transfer are modelled in this algorithm by independent terms of Duhamel's integral. One term is responsible for condensation and the second one for convection, and each of them uses specific temperature response functions calculated with condensation and convection heat transfer coefficient, respectively.

It was shown that the calculation method provides reasonably accurate predictions of casing wall temperature. Comparison of the method predictions with the results of FEM simulations and measurements done at real operating conditions reveals the

same level of accuracy as the finite element method. Relative differences between measured and calculated wall temperatures are within  $(-2.6\%) \div (+1.5\%)$  for the investigated start-ups with condensation and convection heat transfer conditions. This high level of accuracy was achieved by proper determination of temperature response functions which have to be calculated with a variable convection heat transfer coefficient. The quality of results is also improved by applying the constant factor k accounting for nonlinearity of thermal boundary conditions due to the variable heat transfer coefficient at convection.

The advantage of this method are fast and robust temperature calculations as well as its simple mathematical formulation, making it relatively easy for implementation in programmable logic controllers. It should also be emphasised that temperature calculations are performed using only steam temperature as an input without a need of installing metal temperature measurement in the area of interest. Turbine and valve casings are elements of complex geometry, and wall temperature measurements at critical locations are usually difficult in practical realisation. Moreover, in the case of rotating components, like rotors or blades, direct continuous measurements of metal temperature are still impractical and only short-term measurements with the help of optical probes are feasible [44]. Additional difficulty is also related to steam condensation, which reduces the accuracy of optical measurements.

#### References

- [1] European Union. Directorate-General for Energy. (2023). *EU Energy in Figures* [accessed 22 May 2025].
- [2] Rusin, A., Łukowicz, H., Lipka, M., Banaszkiewicz, M., & Radulski, W. (2005). Continuous control and optimisation of thermal stresses in the process of turbine start-up. *Proceedings of the 6th International Congress on Thermal Stresses*, 26–29 May, Vienna, Austria.
- [3] Rusin, A., Radulski, W., & Banaszkiewicz, M. (2001). The Use of Duhamel's Integral in Lifetime Supervision Systems of Steam Turbines. 5th Conference on Research Problems in Power Engineering, 4–7 December, Warsaw, Poland.
- [4] Rusin, A., Łukowicz, H., Malec, A., Banaszkiewicz, M., & Lipka, M. (2003). Optimisation of Start-up Parameters of Steam Turbines. 6th Conference on Research Problems in Power Engineering, 9–12 December, Warsaw, Poland.
- [5] Taler, J., Węglowski, B., Zima, W., Duda, P., Grądziel, S., Sobota, T., Cebula, A., & Taler, D. (2008). Computer system for monitoring power boiler operation. *Proceedings of the Institution of Mechanical Engineers. Part A, Journal of Power and Energy; Journal*, 222, 13–24. doi:10.1243/09576509JPE419
- [6] Lee, H.Y., Kim, J.B., & Yoo, B. (1999). Green's function approach for crack propagation problem subjected to high cycle thermal fatigue loading. *International Journal of Pressure Vessels and Piping*, 76(8), 487–494. doi: 10.1016/S0308-0161(99) 00039-3
- [7] Song, G., Kim, B., & Chang, S. (2011). Fatigue life evaluation for turbine rotor using Green's function. *Proceedia Engineering*, 10, 2292–2297.
- [8] Koo, G.K., Kwon, J.J., & Kim, W. (2009). Green's function method with consideration of temperature dependent material properties for fatigue monitoring of nuclear power plants. *Inter*national Journal of Pressure Vessels and Piping, 86(2–3), 187–195. doi: 10.1016/j.ijpvp.2008.09.006

- [9] Botto, D., Zucca, S., & Gola, M.M. (2003). A methodology for on-line calculation of temperature and thermal stress under nonlinear boundary conditions. *International Journal of Pressure Vessels and Piping*, 80(1), 21–29. doi: 10.1016/S0308-0161(02) 00139-4
- [10] Zhang, H.L., Liu, S., Xie, D., Xiong, Y, Yu. Y., Zhou, Y., & Guo, R. (2013). Online fatigue monitoring models with consideration of temperature dependent properties and varying heat transfer coefficients. *Hindawi Publishing Corporation. Science and Technology of Nuclear Installations*, ID 763175, 1–9. doi: 10.1155/2013/76317
- [11] Rusin, A., Nowak, G., & Lipka, M. (2014). Practical Algorithms for Online Stress Calculations and Heating Process Control. *Jour*nal of Thermal Stresses, 37(11), 1286–1301. doi: 10.1080/ 01495739.2014.937219
- [12] Nowak, G., & Rusin, A. (2016). Using the artificial neural network to control the steam turbine heating process. *Applied Thermal Engineering*. 108, 204–210. doi: 10.1016/j.applthermaleng. 2016.07.129
- [13] Dominiczak, K., Rządkowski, R., Radulski, W., & Szczepanik, S. (2015). Neural networks in stress control system of steam turbine rotor. Wydawnictwo Naukowe Instytutu Technologii Eksploatacji – PIB, 2015 (in Polish).
- [14] Taler, J., Węglowski, B., & Pilarczyk, M. (2017). Monitoring of thermal stresses in pressure components using inverse heat conduction methods. *International Journal of Numerical Methods Heat & Fluid Flow*, 27, 740–756. doi: 10.1108/HFF-03-2016-0091
- [15] Taler, J., Dzierwa, P., Jaremkiewicz, M., Taler, D., Kaczmarski, K., Trojan, M., Węglowski, B., & Sobota, T. (2019). Monitoring of transient 3D temperature distribution and thermal stress in pressure elements based on the wall temperature measurement. *Journal of Thermal Stresses*, 42, 698–724. doi: 10.1080/01495739.2019.1587328
- [16] Pilarczyk, M., & Węglowski, B. (2019). Determination and validation of transient temperature fields within a cylindrical element using the inverse heat conduction method. *Applied Thermal Engineering*, 150, 1224–1232. doi: 10.1016/j.applthermaleng.2019. 01.079
- [17] Węglowski, B., & Pilarczyk, M. (2018). Experimental and numerical verification of transient spatial temperature distribution in thick-walled pressure components. *Journal of Mechanical Science and Technology*, 32, 1087–1098. doi: 10.1007/s12206-018-0211-z.
- [18] Banaszkiewicz, M. (2017). On-line determination of transient thermal stresses in critical steam turbine components using a two-step algorithm. *Journal of Thermal Stresses*, 40(6), 690–703. doi: 10.1080/01495739.2016.1249988
- [19] Banaszkiewicz, M., & Badur, J. (2018). Practical methods for online calculations of thermoelastic stresses in steam turbine components. In *Selected Problems of Contemporary Thermomechanics*, (pp. 45–63), Intech Open. doi: 10.5772/intechopen. 75876
- [20] Taler, J. (1995). *Theory and practice of heat transfer processes identification*. Zakład Narodowy im. Ossolińskich (in Polish).
- [21] Noda, N., Hetnarski, R.B., & Tanigawa, Y. (2003). *Thermal stresses* (2nd edition), Taylor & Francis, New York.
- [22] Zienkiewicz, O.C., Taylor, R.L., & Zhu, J.Z. (2005). The Finite Element Method: It's Basis and Fundamentals. Elsevier Butterworth-Heinemann, Oxford.
- [23] Chmielniak, T., & Kosman, G. (1990). *Thermal loads of steam turbines*. Wydawnictwa Naukowo-Techniczne (in Polish).

- [24] Badur, J., Ziółkowski, P., Kornet, S., Stajnke, M., Bryk, M., Banaś, K., & Ziółkowski, P.J. (2017). The Effort of The Steam Turbine Caused by a Flood Wave Load. In AIP Conference Proceedings. IX Polish National Conference on Applied Mechanics, 25 November, Bydgoszcz, Poland. doi: 10.1063/1.4977675
- [25] Badur, J., Ziółkowski, P., Sławiński, D., & Kornet, S. (2015). An Approach for Estimation of Water Wall Degradation Within Pulverized-Coal Boilers. *Energy*, 92, 142–152. doi: 10.1016/j. energy.2015.04.061
- [26] Badur, J., Ziółkowski, P., Zakrzewski, W., Sławiński, D., Kornet, S., Kowalczyk, T., Hernet, J., Piotrowski, R., Felicjancik, J., & Ziółkowski, P.J. (2015). An advanced Thermal-FSI approach to flow heating/cooling. *Journal of Physics: Conference Series*, 530, 012039. doi: 10.1088/1742-6596/530/1/012039
- [27] Banaś, K., & Badur, J. (2017). Influence of Strength Differential Effect on Material Effort of a Turbine Guide Vane Based on a Thermoelastoplastic Analysis. *Journal of Thermal Stresses*, 40(11), 1368-1385. doi: 10.1080/01495739.2017.1352463
- [28] Gnielinski, V. (1975). Neue Gleichungen für den Wärme- und den Stoffübergang in turbulent durchströmten Rohren und Kanälen. Forschung Ingenieurwes. (Engineering Research), 41, 8–16. doi: 10.1007/BF02559682
- [29] Gnielinski, V. (1976). New equations for heat and mass transfer in the turbulent pipe and channel flow. *International Chemical Engineering*, 16, 359–368.
- [30] Filonienko, G.L. (1954). Friction factor for turbulent pipe flow, *Teploenergetika*, 1(4), 40–44 (in Russian).
- [31] Dittus, F.W., & Boelter, L.M.K. (1930). Heat transfer in automobile radiators of the tubular type. *The University of California Publications on Engineering*, 2, 443–461. (Reprinted in *International Communications in Heat and Mass*, 12, 3–22, 1985).
- [32] Winterton, R.H.S. (1998). Where did the Dittus and Boelter equation come from?. *International Journal of Heat and Mass Transfer*, 41, 809–810. doi: 10.1016/S0017-9310(97)00177-4
- [33] McAdams, W.H. (1954). *Heat Transmission* (3rd ed.), McGraw-Hill, New York.
- [34] Colburn, A.P. (1933). A method of correlating forced convection heat transfer data and a comparison with fluid friction, *Transactions AIChE*, 29, 174–210. (*International Journal of Heat and Mass Transfer*, 7(12), 1359–1384. doi: 10.1016/0017-9310(64) 90125-5).
- [35] Badur, J., & Karcz, M. (2009). Analysis of heat transfer conditions in stop valve chamber of 230 MW turbine. Unpublished report.
- [36] Marinescu, G., Ehrsam, A., Sell, M., & Brunner, P. (2013). Experimental investigation into thermal behaviour of steam turbine components. Part 3 startup and the impact on LCF life. *Proceedings of ASME Turbo Expo*, 3–7 June, San Antonio, USA. doi: 10.1115/GT2013-94356
- [37] Taler, J., & Duda, P. (2006). Solving Direct and Inverse Heat Conduction Problems (pp. 19–20), Springer, Berlin/Heidelberg.
- [38] Pilarczyk, M., Weglowski, B., & Nord, L.O. (2020). A Comprehensive Thermal and Structural Transient Analysis of a Boiler's Steam Outlet Header by Means of a Dedicated Algorithm and FEM Simulation. *Energies*, 13(1), 111. doi: 10.3390/en13010111
- [39] Shah, M.M. (1979). A general correlation for heat transfer during film condensation inside pipes. *International Journal of Heat and Mass Transfer*, 22, 547–556. doi: 10.1016/0017-9310(79)90058-9
- [40] Abaqus User Manual, ver. 6.6.
- [41] DIN EN 10213. (2016). Steel castings for pressure purposes.

- [42] Banaszkiewicz, M. (2016). On-line monitoring and control of thermal stresses in steam turbine rotors, *Applied Thermal Engi*neering, 94, 763–776. doi: 10.1016/j.applthermaleng.2015.10. 131
- [43] Carslaw, H.S., & Jaeger, J.C. (1959). *Conduction of Heat in Solids*, Oxford University Press.
- [44] Marinescu, G., Mohr, W., Ehrsam, A., Ruffino, P., & Sell, M. (2014). Experimental investigation into thermal behaviour of steam turbine components temperature measurements with optical probes and natural cooling analysis. *Journal of Engineering for Gas Turbines and Power*, 136(2), 021602. doi: 10.1115/1. 4025556